THERMAL MODELING AND CORRELATION OF THE SPACE ENVIRONMENTS COMPLEX VACUUM CHAMBER AND CRYOSHROUD

Erik J. Stalcup
NASA Glenn Research Center

ABSTRACT

A thermal model of the Space Environments Complex (SEC) vacuum chamber and cryoshroud has been developed in support of upcoming thermal vacuum/thermal balance testing for Orion EM-1. The model was developed in Thermal Desktop and includes the vacuum chamber itself, a fluid model of the gaseous nitrogen flowing through the cryoshroud and the chamber piping, the Heat Flux System (HFS) within the cryoshroud, and the mechanical ground support equipment (MGSE) that interfaces with the vehicle. It has been correlated with steady state data from three tests. Two tests ran the cryoshroud in hot mode at 170 °F, and one test ran the cryoshroud in cold mode at -263 °F. Correlation was done using an optimization algorithm to find values of unknown contact conductances that minimized the RMS error between the model predictions and the test data. Overall, model quality was very good with a total RMS error of 2.6 °F.

INTRODUCTION

The Space Environments Complex (SEC), formerly known as the Space Power Facility (SPF), is located at Plum Brook Station in Sandusky, Ohio and is a NASA test facility for simulating space environments. It houses a number of large-scale test facilities, including the Space Simulation Vacuum Chamber, the world's largest vacuum chamber. The chamber is 100 ft in diameter and 122 ft high, with a volume of 800,000 ft^3. It is capable of sustaining a vacuum level of less than 2×10^{-6} torr with a pumpdown time of less than 8 hours. The cryoshroud system within the chamber can control the background thermal radiation environment from -250 °F to +140 °F. This is accomplished using a recirculating gaseous nitrogen system, relying on compressors to reach the hot temperatures, and a heat exchanger and liquid nitrogen desuperheater to reach the cold temperatures. A diagram of the Space Simulation Vacuum Chamber is shown in Figure 1.

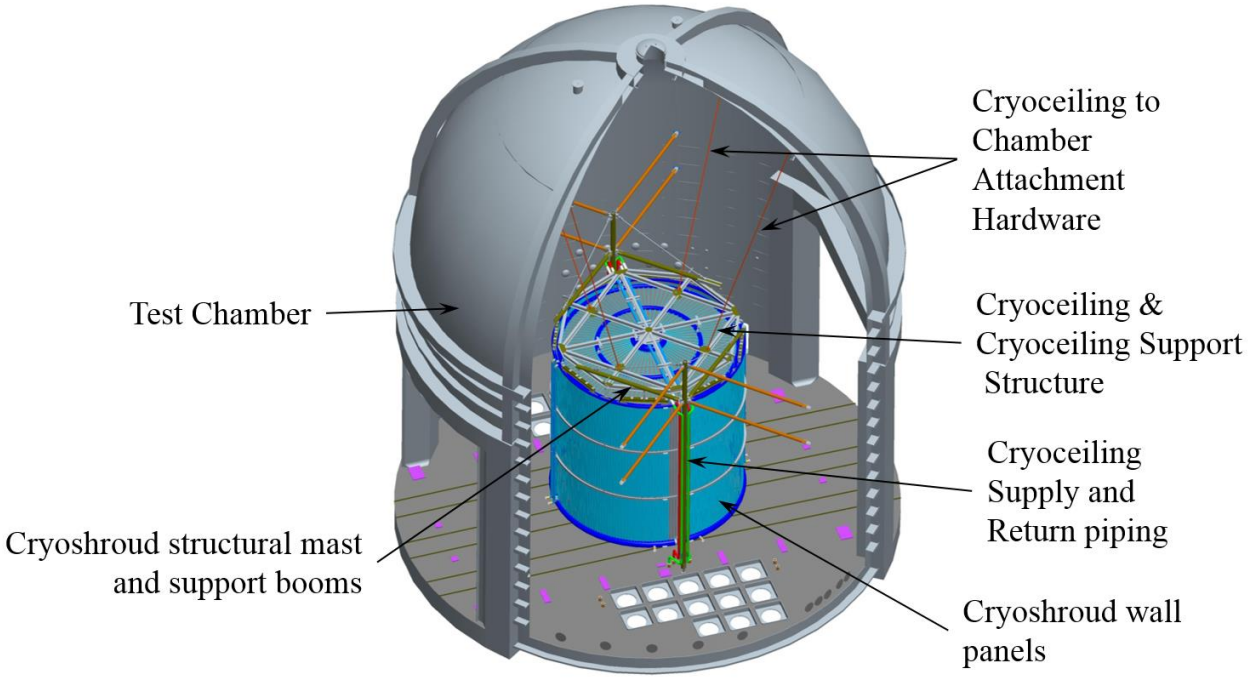

Figure 1. Space Simulation Vacuum Chamber Diagram.

The Space Simulation Vacuum Chamber will be used for the thermal vacuum/thermal balance test for the Orion spacecraft. This test will expose the vehicle to various thermal environments over a period of 60+ days using the cryoshroud as well as the Heat Flux System (HFS), which has been built for this test. The HFS is a structure composed of several zones of radiant heaters that surround the vehicle in order to simulate the space environments that the vehicle would experience in flight. In addition to the HFS, there are a number of other pieces of mechanical ground support equipment (MGSE) that are required for the test, including structural supports for the cryoshroud, HFS, and vehicle.

A Thermal Desktop model of the vacuum chamber, the cryoshroud, the HFS, and the MGSE has been developed in anticipation of the Orion EM-1 thermal vacuum/thermal balance test. This model was primarily created to gain a better understanding of the facility-side systems during a test, however the model has incorporated a version of the Orion Integrated Thermal Model (ITM) (not shown in this document) and is capable of simulating the full test with a detailed vehicle model. Two of the primary uses of the model are:

1. Predicting MGSE temperatures, to provide input to structural analysis and to evaluate the environment that other test equipment, such as cable harnesses, might be exposed to
2. Predicting the heat load on the gaseous nitrogen system

This document details the steady state correlation of this model using data from multiple system tests run at various operating conditions.

MODEL DESCRIPTION

An overview of the model geometry is shown in Figure 3. Each component of the system is shown sequentially and is described as follows:

a. Cryofloor Transfer Cart (CTC): The CTC supports the weight of the cryofloor, MGSE, and the vehicle. It is composed of I-beams and rolls along rails on the chamber floor.

b. Cryofloor: The cryofloor rests on top of the CTC, separated by plastic isolators. The cryofloor itself is an array of extruded tubes with inlet and outlet manifolds. A cross-section showing the shape of the extruded tubes and the isolators is shown in Figure 2

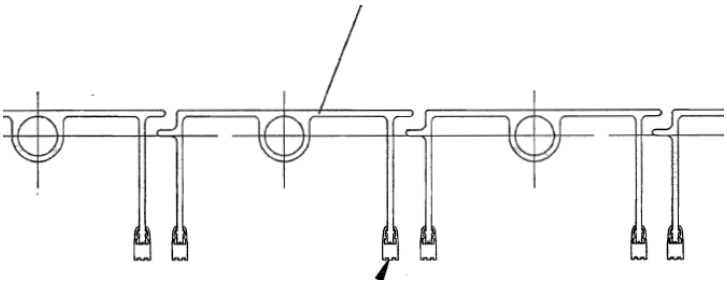

Figure 2. Cryofloor extrusion and isolators.

c. Flat Beam Interface (FBI) and Cryofloor Interface Adapter (CIA): The FBI and CIA are structural elements composed of I-beams that support other MGSE. The FBI supports the Thermal Enclosure Structure (TES), a part of the HFS described later, and the CIA ultimately supports the vehicle. Both of these interface with the CTC through penetrations in the cryofloor and therefore do not directly contact the cryofloor.

d. Cone Spacer Stand (CSS): The CSS sits on top of the CIA and is another piece of structure that supports the vehicle.

e. Aft heat plates: The aft heat plates are one part of the HFS and provide radiant heat to the aft portions of the vehicle. The vertical plates are attached to the CSS and the horizontal plates are attached to the CIA.

f. Umbilical masts: The umbilical masts are attached to the CSS using brackets. These primarily support various cable harnesses.

g. Aft ring: The aft ring sits on top of the CSS and is the direct attachment point for the vehicle.

h. Thermal Enclosure Structure (TES): The TES is the other part of the HFS, providing radiant heat to the forward portions of the vehicle. It is separated into two “clam shells” that roll along the FBI rails to create the enclosure.

i. Cryowalls, cryoceiling, supply/return pipes: These comprise the remainder of the cryoshroud system inside the chamber. The cryowalls and cryoceiling are suspended above the cryofloor with support structures, most of which are not modeled. Both the cryowalls and cryoceiling are divided into four separate zones, each with an inlet and outlet manifold for the gaseous nitrogen piping. The cryowall piping is made up of extruded tubes, similar to the cryofloor. The cryoceiling piping is made up of tubes that

Figure 3. Model Geometry.

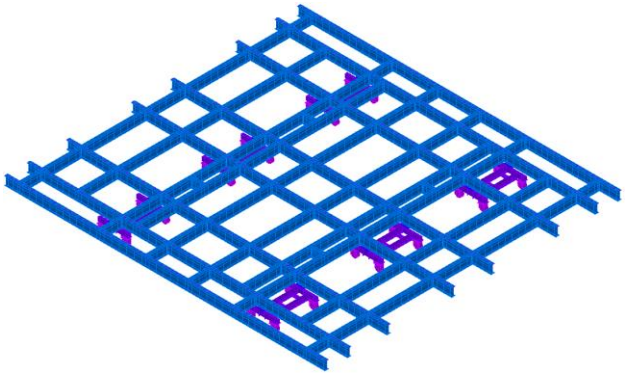

(a) CTC

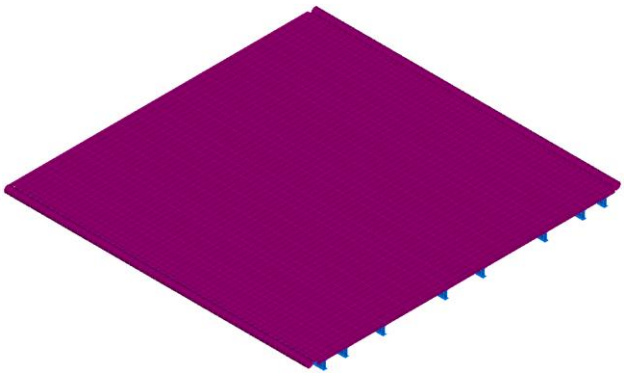

(b) Cryofloor

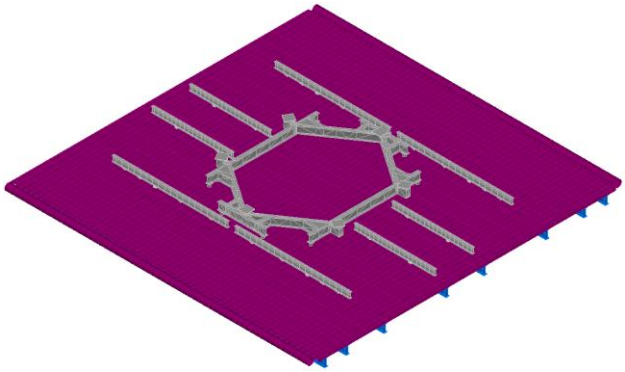

(c) FBI and CIA

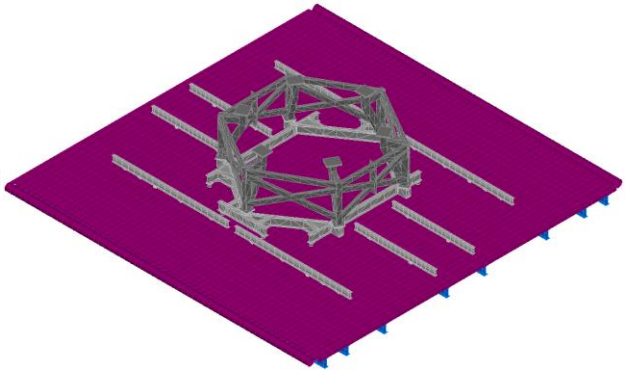

(d) CSS

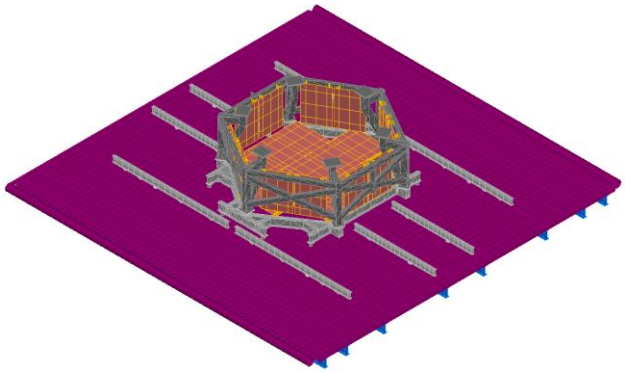

(e) Aft heat plates

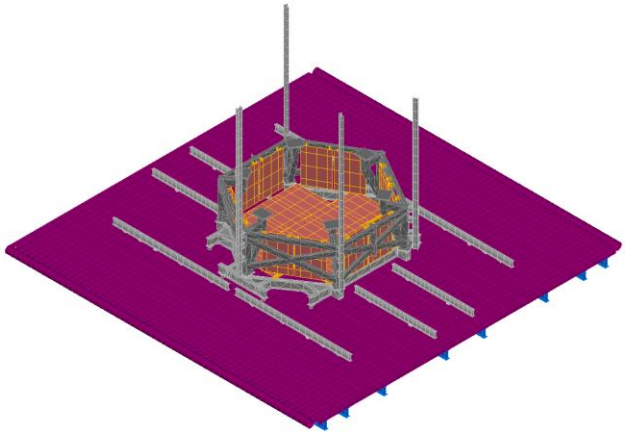

(f) Umbilical masts

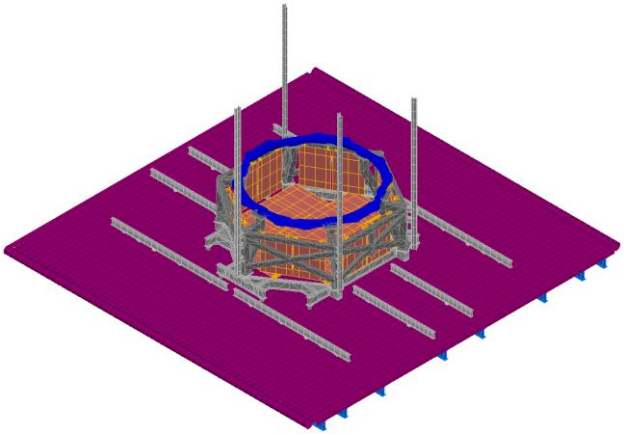

(g) Aft ring

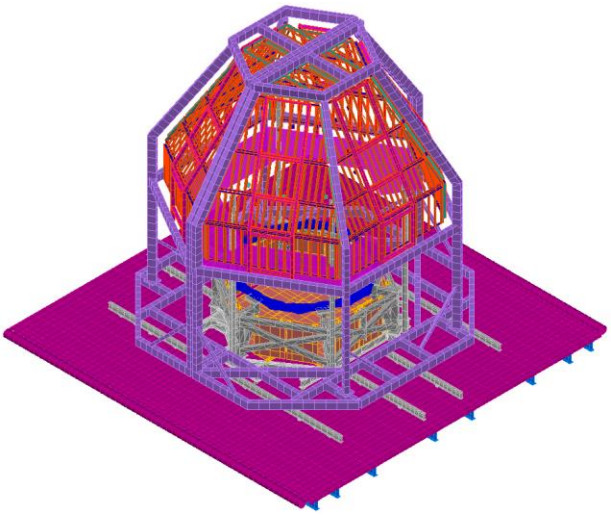

(h) TES

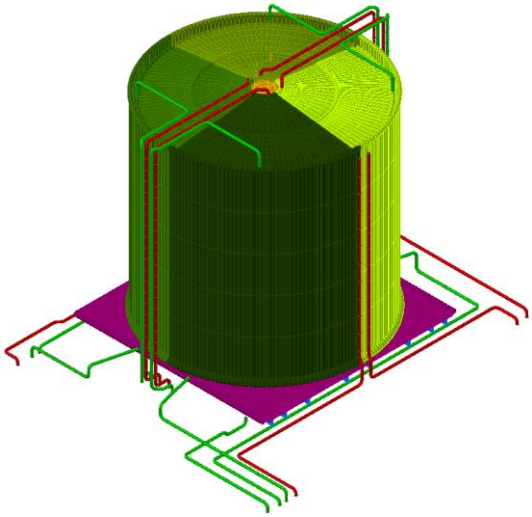

(i) Cryowalls, cryoceiling, supply/return pipes

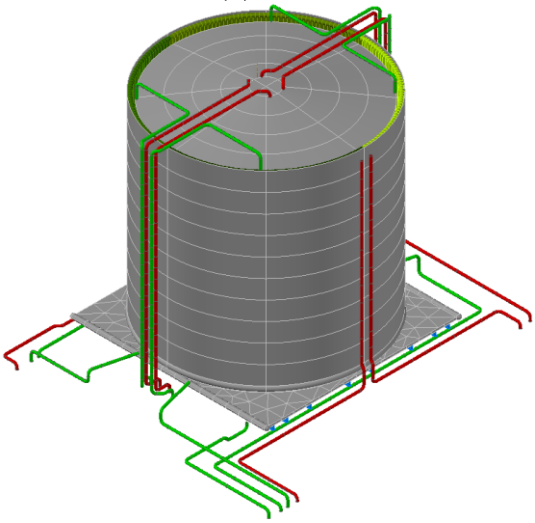

(j) Insulation

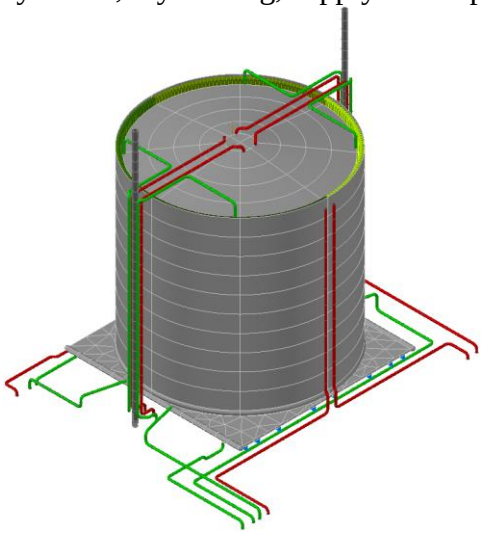

(k) Masts

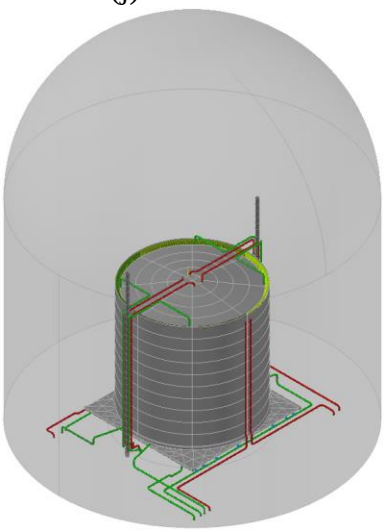

(l) Chamber

are welded to plates. In order to provide a path for air to exit the interior of the shroud during pump down before the test, and to allow for outgassing during the test, there is a gap between the cryowalls and the cryoceiling. This is an important feature to model accurately as it also represents a radiative coupling between the warm chamber walls and the interior of the cryoshroud. Also shown are the supply/return pipes that connect to the inlet and outlet manifolds of each zone of the cryoshroud.

j. Insulation: A single layer of double-aluminized Mylar (DAM) surrounds the cryoshroud (without covering the gap between the cryowalls and cryoceiling) in order to reduce radiative heat transfer from the vacuum chamber. There are also two sheets of double-aluminized Mylar below the cryofloor – one between the cryofloor and the isolators, and one between the isolators and the CTC.

k. Masts: The masts are a part of the assembly that suspends the cryowalls and are attached to the chamber floor.

l. Chamber: This represents the vacuum chamber itself, which surrounds the entire system.

The model was developed in Thermal Desktop 5.8, utilizing RadCAD for radiation calculations and FloCAD for the gaseous nitrogen fluid model. It contains 29,265 nodes and 55,165 linear conductors. The gaseous nitrogen fluid model contains 4,870 lumps, 5,301 paths, and 4,059 ties. Most components were modeled using TD primitives, but the CIA, CSS, and aft ring were meshed and imported with SpaceClaim.

Included in the model are 93 Temperature Measures meant to represent test thermocouples. Of these, 81 are on the cryoshroud and the remainder is on MGSE. Additionally, there are 3 radiation sink nodes (4 in diameter spheres) that represent test thermocouples used to measure the radiative environment. These thermocouples are attached to long chains that are suspended from support structure above. The chains are not modeled, as it is assumed that conduction through that path is negligible.

Boundary conditions include the chamber temperatures, and gaseous nitrogen temperature, pressure, and flow rates.

INTEGRATED SYSTEM TEST MODEL CORRELATION

In January 2014 and August 2015, two Integrated System Tests (ISTs) were performed in the "empty chamber" configuration, in which the cryoshroud was operated without any of the previously mentioned MGSE inside. For the January 2014 test, the cryoshroud was operated at 170 °F for approximately 37 hours. Insulation was installed as described above. For the August 2015 test, the cryoshroud was operated at 170 °F for 14 days. Insulation was not installed for this test. Data from the ends of both of these tests were used for correlation of the model. Both tests took measurements from the 81 thermocouples on the cryoshroud, however, 13 thermocouples in the January 2014 test produced bad readings and were not used for model comparison.

Model results for both tests are shown in Figure 4-Figure 6, for the cryofloor, one cryowall zone, and one cryoceiling zone. In general, the model predictions and the test data agreed very well, with the exception of the intermediate header manifold on the cryoceiling. This is visible as the

dark blue cold section of Figure 6. The fluid network representing this manifold is shown in Figure 7. The model predicts regions of zero flow, as the gaseous nitrogen takes the shortest path from the inlets (bottom of the figure) to the outlets (top of the figure). In reality, the flow behavior inside the manifold is very complex and largely unknown. There may be significant three-dimensional effects that FloCAD cannot capture with one-dimensional flow modeling. Regions of stagnant flow may be present, but would likely be more localized. Therefore, the heat transfer from the gaseous nitrogen to the manifold piping is under predicted. Adding a multiplier of 5 to the heat transfer coefficient resulted in much better agreement with the test data. No other changes were made for model correlation.

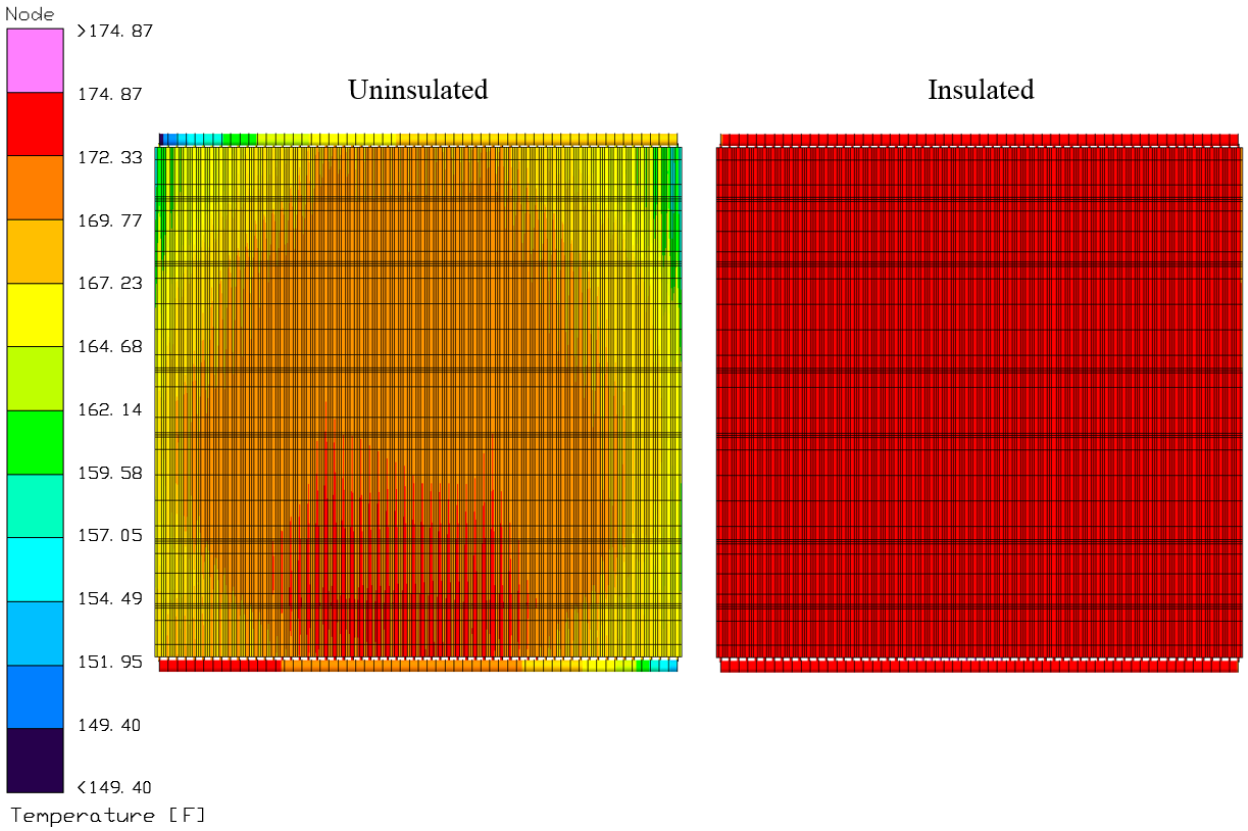

Figure 4. IST model results for the cryofloor.

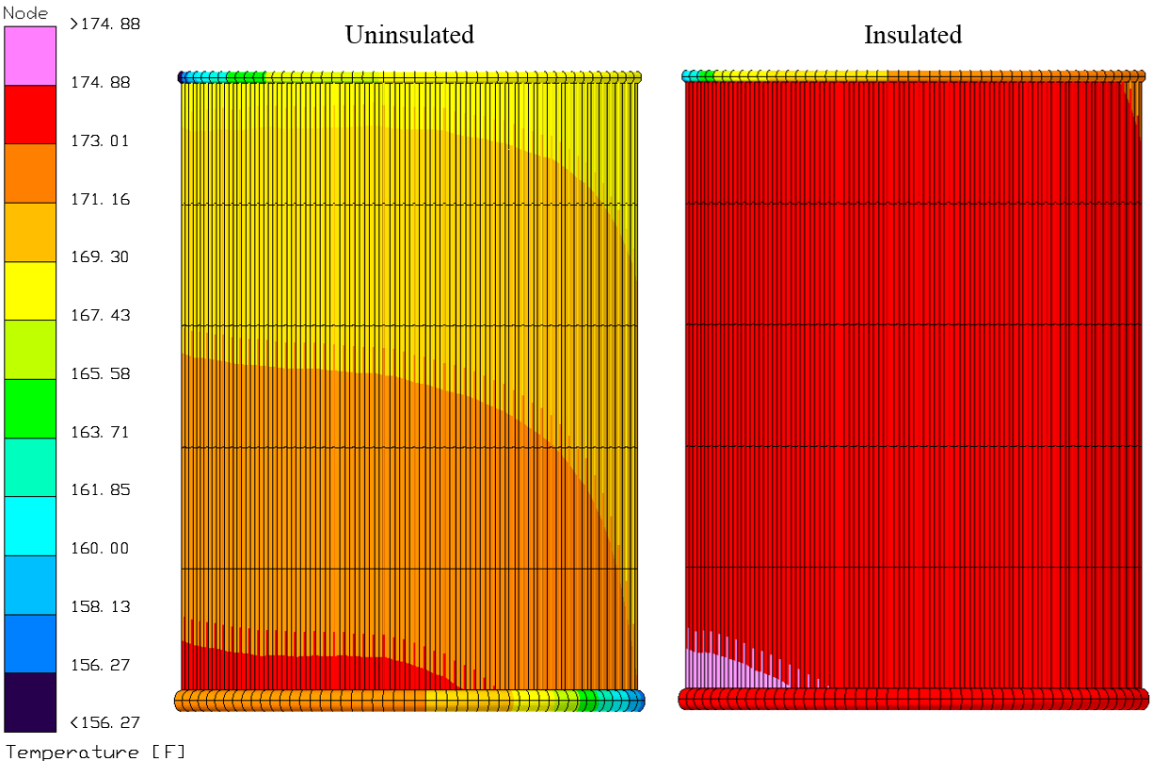

Figure 5. IST model results for the southeast cryowall.

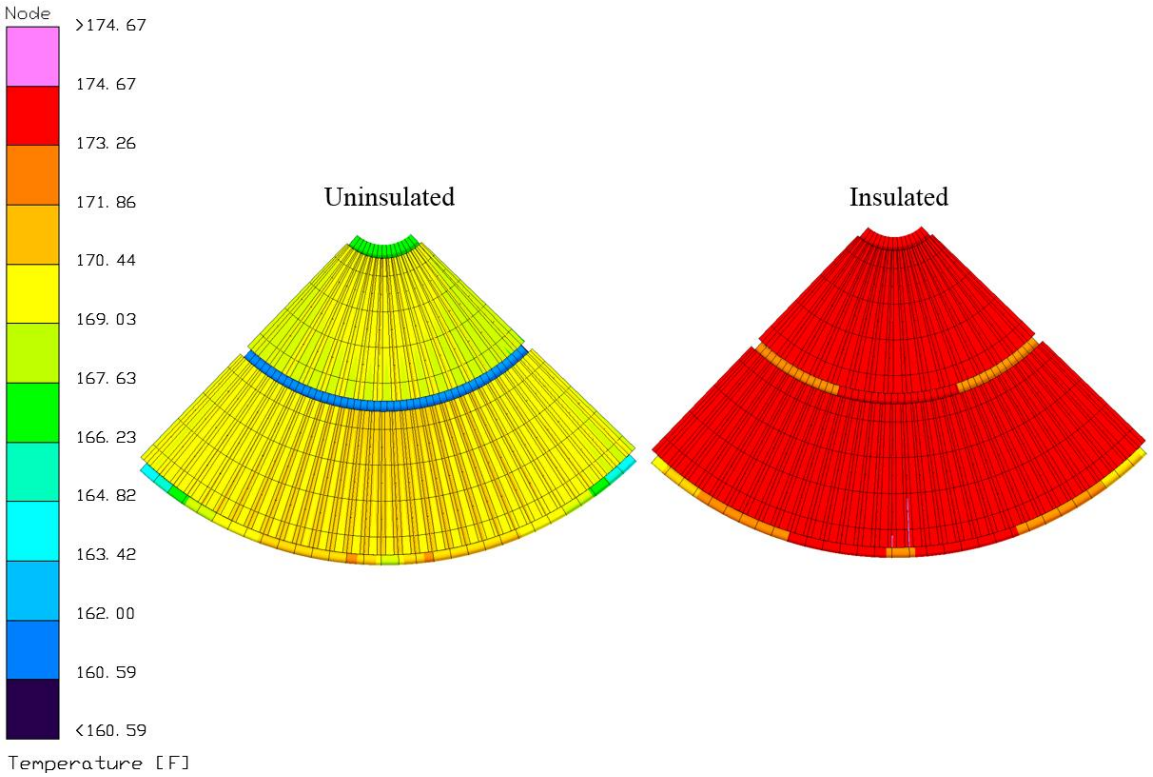

Figure 6. IST model results for the southeast cryoceiling.

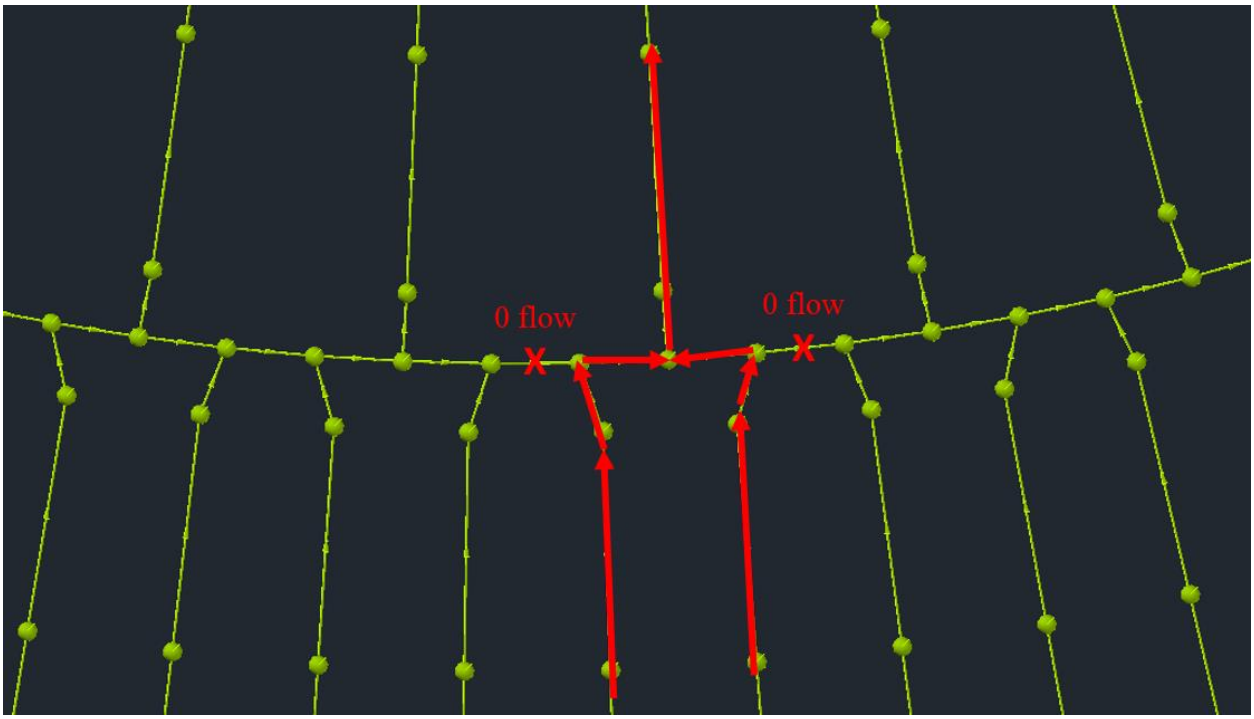

Figure 7. Cryoceiling intermediate header manifold flow network.

A summary of the correlation errors is shown in Table 1. Predictions for both the insulated January 2014 test and the uninsulated August 2015 test showed good correlation with the data.

Table 1. IST Model Correlation Errors

	January 2014 IST (Insulated)	August 2015 IST (Uninsulated)
Average Error (°F)	**0.3**	**0.6**
RMS Error (°F)	**1.1**	**3.7**

BAKE-OUT TEST MODEL CORRELATION

In May 2018, the SEC Thermal Vacuum Bake-out Test was performed in order to collect data related to chamber and cryoshroud cleanliness, pressure environments, and operations prior to the Orion EM-1 thermal vacuum/thermal balance test. Thermocouple and gaseous nitrogen data were also collected, providing a dataset for model correlation. In the bake-out configuration, the only MGSE present inside the cryoshroud were the CIA and FBI, as shown in Figure 3c. The cryoshroud itself, including the insulation, is configured as previously described (Figure 3l). A pair of scavenger plates, two LED lamp/camera assemblies, and various contamination monitoring devices were also present inside the cryoshroud during bake-out but were not modeled. The test consisted of several hot and cold plateaus. The data used for this correlation is from the end of 3 days of operation at approximately -263 °F.

Although the bake-out dataset does not include all the MGSE that will be present during the thermal vacuum test, it does contain valuable data for improving the modeling of the insulation and the refining contact conductances between the MGSE that was present. To that end, the following correlation approach was taken:

1. Reevaluate the cryoshroud predictions, as several modifications were made after correlation with the ISTs.
2. Adjust contact conductances for MGSE inside and in contact with the cryoshroud.
3. Adjust insulation and contact conductances for MGSE outside the cryoshroud.

After correlation with the ISTs, several changes were made to the fluid model, which necessitated a reevaluation of the cryoshroud predictions. Changes included repositioning where the supply/return lines connect to the inlet/outlet header manifolds and modifying the frictional flow losses. Model results for the bake-out gave an RMS error of 1.6 °F for the 81 cryoshroud thermocouples. Though this is higher than the RMS error for the January 2014 insulated IST, it still indicates a very good correlation with no further adjustments needed.

After verifying that the cryoshroud predictions were still well correlated, contact conductances for the MGSE inside the cryoshroud were adjusted. This correlation used data from 12 thermocouples on the CTC, CIA, FBI, and cryofloor. The contact conductances that were adjusted were between: 1) the FBI and the CTC, 2) the CIA and the CTC, 3) the cryofloor and the CTC (via the isolators), and 4) the CTC and the chamber floor (via the dolly assemblies). These are shown in Figure 8, with contact conductances indicated by resistor symbols. These represent some of the largest sources of uncertainty in the model. To find the best values for the conductances, optimization algorithms within SINDA/FLUINT were utilized.

The optimization algorithms within SINDA/FLUINT (referred to as the Solver) can be called from Thermal Desktop to seek values of unknown parameters in order to produce the best fit to test data. For this model, the four contact conductances above were input as adjustable parameters with upper and lower limits on their values. The optimization was run using the BFGS iterative method to minimize the RMS error for the 12 thermocouples on these structures. The resulting contact conductances were $H_{FBI-CTC} = 65\ W/m^2/K$, $H_{CIA-CTC} = 53\ W/m^2/K$, $H_{cryofloor-CTC} = 0.31\ W/m^2/K$, and $H_{CTC-chamber} = 98\ W/m^2/K$. The RMS error was 5.3 °F.

One source of error may be the assumption that the contact conductance between the cryofloor and the CTC is the same at each point of contact. It has been observed during cold tests that the cryofloor tends to bow up at the edges. This causes complete loss of contact at the edges and consequently increases the contact pressure near the center. This could clearly have an effect on the temperature distribution throughout the CTC. Other sources of error may be due to ground support equipment that was present during the test but not modeled. This includes two scavenger plates held at temperatures colder than the shroud, and two heated camera/LED lamp assemblies. However, these items are relatively small so their impact may be negligible.

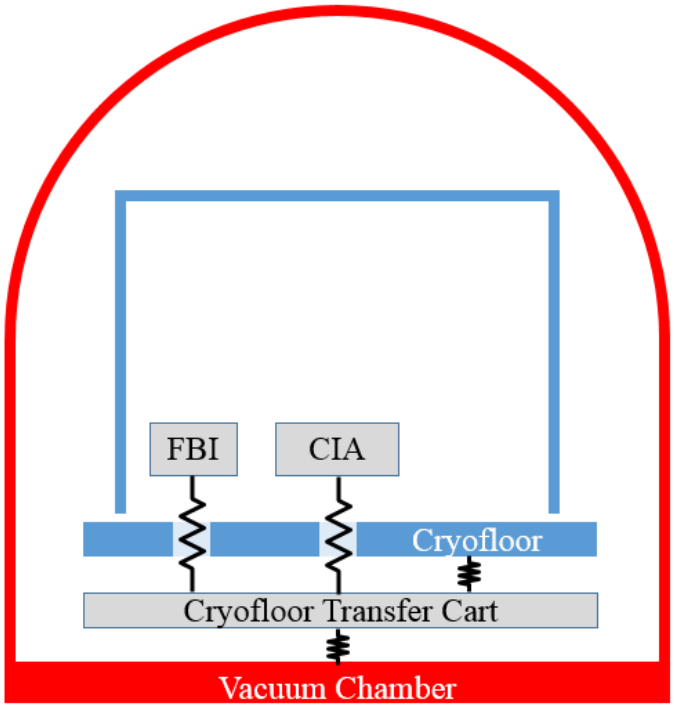

Figure 8. Contact conductance diagram.

The final step for correlation was to adjust insulation and contact conductances for MGSE outside the cryoshroud. Data from three thermocouples were available. Two thermocouples were on the masts, and one thermocouple was attached to a long chain that was suspended from support structure above, acting as a radiative sink. Uncorrelated results indicated that the model was predicting much higher temperatures for these thermocouples. Therefore, the first attempt at correlation was to raise the DAM emissivity from 0.05 to 0.10. However, this had little effect. An examination of the as-installed insulation showed that there was significant contact between it and the cryoshroud, especially on the header manifolds and the cryofloor. This is shown in Figure 9. Additionally, there were areas of incomplete coverage, particularly around the supply/return lines. To capture the reduction in insulation effectiveness due to surface contact and incomplete coverage, a contactor was added between all insulation and the underlying cryoshroud surfaces.

The SINDA/FLUINT optimization algorithms were utilized again, with adjustable parameters of contact conductance between the insulation and the cryoshroud, and the masts and the chamber floor. The resulting contact conductances were $H_{DAM-shroud} = 25\ W/m^2/K$ and $H_{mast-chamber} = 1.0\ W/m^2/K$. The RMS error was 5.0 °F.

One source of error for these predictions is the assumption that the contact conductance between the insulation and the cryoshroud is the same everywhere. Additionally, the small number of test data points for chamber temperatures is a source of error. There were only three thermocouples on the chamber walls and floor and these were used as boundary conditions in the model. In reality, the chamber temperatures will be much less uniform than the model assumes.

A summary of the model correlation errors is shown in Table 2.

Figure 9. Vacuum chamber and cryoshroud prior to bake-out.

Table 2. Bake-out Model Correlation Errors

	Cryoshroud (81 TCs)	Interior (12 TCs)	Exterior (3 TCs)	**Total (96 TCs)**
Average Error (°F)	-0.9	0.1	4.7	**-0.3**
RMS Error (°F)	1.6	5.3	5.0	**2.6**

CONCLUSIONS

In summary, the SEC vacuum chamber and cryoshroud model is very well correlated with a total RMS error of 2.6 °F. Utilization of the SINDA/FLUINT optimization algorithms and TD Temperature Measures proved to be an effective and efficient method of determining unknown parameters that aided in model correlation. Future work includes performing a transient correlation with the bake-out data, which includes hot and cold plateaus.

ACKNOWLEDGEMENTS

Thanks to the thermal team at NASA GRC and Plum Brook: Jim Yuko, Barbara Sakowski, Jarred Wilhite, Henry Speier, and Erin Reed. Thanks to Justin Elchert and Katie Oriti who developed earlier versions of this model.

ACRONYMS

CIA Cryofloor Interface Adapter

CSS Cone Spacer Stand

CTC Cryofloor Transfer Cart

DAM Double-aluminized Mylar

FBI Flat Beam Interface

HFS Heat Flux System

IST Integrated System Test

ITM Integrated Thermal Model

MGSE Mechanical ground support equipment

SEC Space Environments Complex

SPF Space Power Facility

TD Thermal Desktop

TES Thermal Enclosure Structure